ORIGINAL ARTICLE
DOI: 10.5433/1679-0375.2019v40n2p115

The influence of synthesis temperature on the HT-$LiCoO_2$ crystallographic properties

A influência da temperatura de síntese nas propriedades cristalográficas da fase HT-$LiCoO_2$

Diego Viscovini de Carvalho Sallas[1]; Bianca Akemi Kawata[2]; Olívio Fernandes Galão[3]; Luciana Gomes Chagas[4]; Paulo Rogério Catarini da Silva[5]; Maria Gabriella Detone Guaita[6]; Alexandre Urbano[7]

Abstract

Much of the success of cobalt-based lithium-ion batteries is due to the easy synthesis of HT-$LiCoO_2$ achieved with sol-gel routes. Many sol-gel routes reduced the synthesis temperature from 900 °C - for solid state routes - to 600 °C. To obtain the HT-LCO compound by a chemical route at moderate calcination temperatures, the heating rate at the early stage of the synthesis should be high. However, at high heating rates, a high concentration of energy develops due to the combustion of chelating agents, causing an undesirable great volumetric expansion. Therefore, as a way of minimizing the volumetric expansion effects the heating rate in the synthesis was investigated. X-ray diffraction results showed that using a low heating rate the HT-LCO phase formation requires more than the energy available at 600 °C to be pure and to crystallize in the desired space group. However, for the calcination temperature of 800 °C, only 20 min was sufficient to synthesize a high ordered crystallographic HT-LCO phase. The reduced synthesis time is possibly associated with a high homogenization of the metallic ions since the gel expansion is radically reduced. The LCO synthesized at 800 °C for only 20 min showed electrochemical charge capacity of about 140 mAh g^{-1}. It was concluded that by controlling the kinetics during the heating step, in the early stage of the synthesis, the HT-LCO is obtained with high ordered crystallography, although the synthesis time is reduced, therefore enabling a more economically attractive synthesis process.

Keywords: Lithium batteries. Sol-gel synthesis. $LiCoO_2$. Crystallography. Crystallite size. Micro-strain.

Resumo

Grande parte do sucesso das baterias de íon-lítio à base de cobalto se deve à fácil síntese do HT-$LiCoO_2$ por rotas sol-gel. Muitas rotas sol-gel reduziram a temperatura de síntese de 900 °C - para rotas de estado sólido - para 600 °C. No entanto, para se obter o composto HT-LCO por uma via química a temperaturas de calcinação moderadas, a taxa de aquecimento no estágio inicial da síntese deve ser alta. Em altas taxas de aquecimento, uma alta concentração de energia se desenvolve devido à combustão do agente quelante, causando uma grande e indesejável expansão volumétrica. Portanto, como forma de minimizar os efeitos da expansão volumétrica, a taxa de aquecimento na síntese foi investigada. Os resultados da difração de raios X mostraram que, usando uma baixa taxa de aquecimento, a formação da fase HT-LCO exige que mais do que a energia disponível a 600 °C para ser pura e se cristalize no grupo espacial desejado. No entanto, para a temperatura de calcinação de 800 °C, apenas 20 minutos foram suficientes para sintetizar uma fase HT-LCO cristalográfica com alto ordenamento. O tempo de síntese reduzido está possivelmente associado a uma alta homogeneização dos íons metálicos, uma vez que a expansão do gel é radicalmente reduzida. O LCO sintetizado a 800 °C por apenas 20 min mostrou capacidade de carga eletroquímica de cerca de 140 mAh g^{-1}. Conclui-se que, controlando a cinética durante a etapa de aquecimento, na fase inicial da síntese, o HT-LCO é obtido com alto ordenamento cristalográfico, embora o tempo de síntese seja reduzido, possibilitando um processo de síntese economicamente mais atraente.

Palavras-chave: Baterias de íon-lítio. Síntese sol-gel. $LiCoO_2$. Cristalografia. Tamanho de cristalito. Micro-deformação.

[1] Dept. Química, UEL, Londrina, Pr, Brasil; E-mail: diegosallas@gmail.com
[2] MSc., Dept. Física, UEL, Londrina, Pr, Brasil; E-mail: a.kawata@hotmail.com
[3] Prof. Dr., Dept. Química, UEL, Londrina, Pr, Brasil; E-mail: galao@uel.br
[4] Dra., Johnson Matthey, Blount's Court, Sonning Common, United Kingdom; E-mail: Luciana.GomesChagas@matthey.com
[5] Dr., Dept. Física, UEL, Londrina, Pr, Brasil; E-mail: prcsilva@uel.br
[6] Dept. Química, UEL, Londrina, Pr, Brasil; E-mail: gabriellaguaita@hotmail.com
[7] Prof. Dr., Dept. Física, UEL, Londrina, Pr, Brasil; E-mail: aurbano@uel.br]

Introduction

Lithium cobalt oxide ($LiCoO_2$, LCO) has been successfully used as the electroactive material on the positive electrode of lithium-ion batteries (LIBs) since the 1990s (MIZUSHIMA *et al*., 1981). This predominance is mainly due to its high specific gravimetric (Wh g^{-1}) and volumetric (Wh L^{-1}) energy capacities and extended cycle life. These properties allow high-energy batteries to be built in low volume and low weight, which is suitable for equipping wireless electronic devices and electric vehicles (JULIEN, 2000; LI *et al*., 2018). On the other hand, the sol-gel synthesis route contributes greatly to improving the cost-benefit for commercial production (CHEN *et al*., 2002; GUMMOW *et al*., 1992). The sol-gel route has been widely explored and has the advantages of low cost and small particle size production. As the smaller is the particle size, higher is the surface area and faster is the charge recombination in the particle surface (BAZITO; TORRESI, 2006; KIM; LEE; KIM, 2010; OH; HONG; SUN, 1997; ZHU *et al*., 2010). By sol-gel synthesis, the low temperature LCO phase (LT-) can be obtained at 400 °C with crystallographic structure *Fd-3m* or the high temperature phase (HT-LCO) at moderate (600 °C) to high (700-800 °C) calcination temperatures and *R-3m* structure (KANG *et al*., 1999). The LT-LCO phase presents disadvantages when compared to the HT-LCO phase as the low chemical stability in organic electrolytes and the low lithium ion diffusion coefficient (GARCIA; FARCY; PEREIRA-RAMOS; BAFFIER, 1997). The HT-LCO phase, in addition to the chemical stability and the high ion transport coefficient, exhibits a high chargeability of approximately 140 mAh g^{-1} since it has high crystallographic ordering (ANTOLINI, 2004; BELOV; YANG, 2008; KHOMANE *et al*., 2008).

Several types of synthesis have been proposed for the preparation of the HT-LCO phase with different cobalt and lithium precursors and different chelating agents (PORTHAULT *et al*., 2012; PREDOANĂ *et al*., 2007). Among the variations of Pechini sol-gel synthesis, we highlight the one described by Kook and co-authors which employs lithium and cobalt nitrates and the cheap polyacrylic acid (PAA) (SUN, 1999). According to Sun *et al*., polyacrylic acid not only acts as a chelating agent in the sol-gel formation but also provides the combustion heat required to form the HT-LCO phase even at moderate calcination temperatures (600 °C). The use of PAA as a chelating agent, however, presents a significant drawback that is excessive volumetric expansion during the pre-calcination stage, which occurs due to its decomposition and consequent release of gases such as CO and CO_2. Other routes of the chemical solution are proposed in the literature for the synthesis of HT-$LiCoO_2$ aiming to improve the route described by Sun, ruling out the need of pH control and minimizing the volumetric expansion of the material. In these works, the synthesis temperatures were from moderate to high (from 600 °C to 800 °C) and the synthesis time varies from 1 to 10 hours (DING; GE; CHEN, 2005; DONG *et al*., 2011; PORTHAULT; LE CRAS; FRANGER, 2010; YOON; LEE; KIM, 2001; ZHECHEVA *et al*., 1996). In order to minimize the effects of the PAA combustion, in this work, the effect of the heating rate on the crystallographic ordered HT-LCO compound was investigated. In this work were observed that the HT-LCO phase, with the desired crystalline structure for application as electroactive material in LIBs, was obtained at 800 °C with calcination time drastically reduced to 20 minutes if compared to the traditional synthesis.

Methodology

The methodology used for the synthesis of HT-LCO was previously reported by Sun and co-authors (SUN; OH; HONG, 1996), using a 1:1 molar ratio between polyacrylic acid and lithium (or cobalt) ions present in the aqueous solution. The polyacrylic acid and the nitrates used were from Sigma Aldrich *pro analyze*. Thermogravimetric analysis of the precursor gel was performed using Shimadzu's TGA-50 to diagnose the temperatures of weight loss.

For the synthesis, the samples were heat treated with a slow heating ramp of 5 °C min^{-1} until 450 °C, kept at this temperature for 1 hour, and let to cool down. The resulting powder was then macerated and heated with heating ramp of 10 °C min^{-1} until 600 °C, 700 °C or 800 °C. Samples were kept at high temperature for 1 h and 20 h. Besides, for sample heat-treated at 800 °C, it was tested on a reduced time of 20 min. All experiments were conducted in air.

The crystallographic characterization was performed by X-ray powder diffraction (XRD) in an X'Pert PRO diffractometer from PANalytical with Cu K-α radiation (λ = 1.540 Å) in the range of 15 to 75° 2theta. Rietveld refinement (PANalytical X'Pert HighScore Plus software version 2.2d) was used to quantify the crystalline phases and structural parameters (lattice parameters, FWHM, crystallite size, and micro-strain). The crystallographic information cards used for the Rietveld refinement were

29225-ICSD for HT-$LiCoO_2$ (*R-3m*), 74332-ICSD for LT-$LiCoO_2$ (*Fd-3m*) and 69133-ICSD for Li_2CO_3 (*C12/c1*). Polycrystalline silicon was defined as the reference for the instrumental standard used on the calculation of crystallite size and micro-strain.

Crystallite size (D) and micro-strain (ε) were calculated according to equation (1) and (2)

$$D = \frac{180}{\pi} \frac{\lambda}{(W - W_{std})^{1/2}}, \quad (1)$$

$$\varepsilon = \frac{[(U - U_{std}) - (W - W_{std})]^{1/2}}{4.4}. \quad (2)$$

In equations (1) and (2), W and U are the Cagliotti parameters from the $FWHM$ function described in equation (3)

$$FWHM = (Utg^2\theta + Vtg\theta + W)^{1/2}. \quad (3)$$

The width and shape of a diffraction peak are a convolution of the instrumental broadening and the broadening arising from the sample. The sample contribution stems from micro-strain broadening and from crystallite size broadening. Both effects vary as a function of 2θ but in different ways. This allows discriminating between them.

For electrochemical characterization, the electrode was prepared by mixing synthesized HT-LCO, PVDF (Sigma Adrich) and graphite (Nacional de Grafite - Brazil), in an 80:10:10 weight ratio, dissolved in NMP (Acros Organics). The slurry was casted onto an aluminum foil using a doctor blade. The electrode mass was estimated from the average of ten similar electrodes weighed together, resulting in 0.0030 g $\pm$ 0.0005 g per electrode (the mass error was who determine the discharge capacity error). The electrode was dried on a vacuum furnace at 120 °C for 10 h. A two-electrode cell was mounted, and lithium metal (Sigma Aldrich) was used as counter and as reference electrode. The electrolyte was $LiClO_4$/EC-DMC 1:1 (1 M) (Sigma Aldrich) soaked in the hydrophobic paper (Whatman). The electrochemistry was analyzed in an Arbin Instruments battery cycler using the CC-CV protocol. At the CC stage, the applied current was 0.5C (50 μA) between 4.20 to 3.60 V vs. $Li^+|Li$. At the CV stage, the cell remains at upper or lower potential until the current reach 0.010 C.

Results and discussions

From the TGA result shown in Figure 1, four regions of mass loss are observed. The first and second, located near 60 °C and 130 °C respectively, corresponding to the evaporation of water present in the gel. The other two regions, located close to 180 °C and 400 °C, respectively, describe the decomposition of inorganic and organic compounds, resulting in the emission of CO and CO_2.

Based on that, 450 °C as defined as the temperature in which the pre-calcination was completed since no further mass loss was observed. The total gel mass loss was 89%.

Figure 1 – Thermogravimetric analysis of the precursor gel having the chelating agent polyacrylic acid.

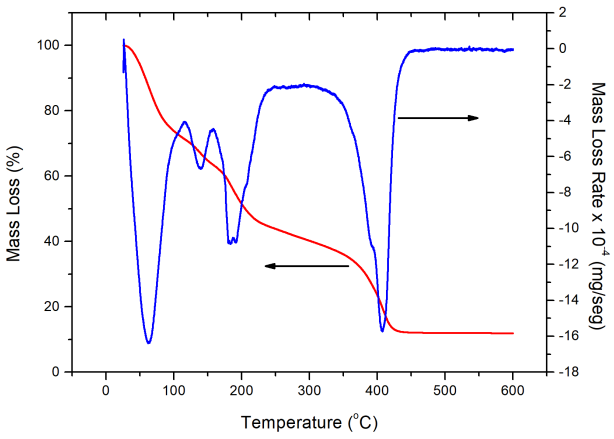

Source: The authors.

Figure 2 shows the diffractograms from samples calcined at 600, 700 and 800 °C at different times. In all sample the *R-3m* hexagonal crystallographic phase (HT-LCO) is present.

Figure 2 – Diffractogram from LCO samples: (a) 600 °C - 1 h, (b) 600 °C - 20 h, (c) 700 °C - 1 h, (d) 700 °C - 20 h, (e) 800 °C - 20 min, (f) 800 °C - 1 h, (g) 800 °C - 20h.

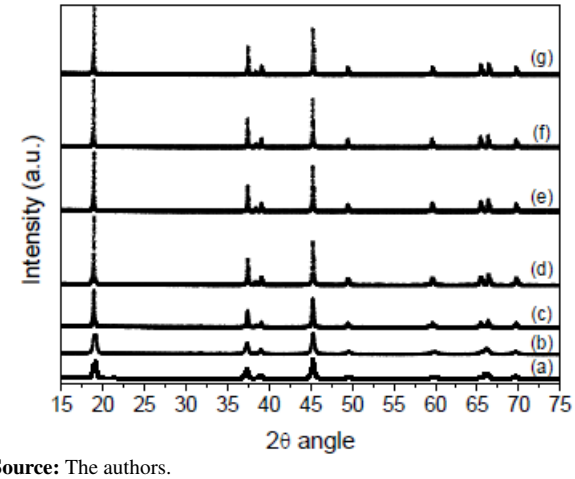

Source: The authors.

In the presented scale in Figure 2, the main difference between the diffractograms were the peak *FWHM* enlargements for the 600 °C samples (2a and 2b) and the ratio between (003) and (104) peak intensities for HT-LCO,

which was around or greater than 1.2 for the 700 °C-1h to 800 °C-20h samples (2c to 2g). The relative peak enlargement is characteristic of the decrease in the crystallite size and increase of the micro-strain (crystal disorder). For HT-LCO phase when the (003)/(104) peak intensity ratio is higher than 1.2, it is an indicator that there is an ordered lamellar ionic disposition, in which cobalt occupy the 3b Wyckoff site (HU *et al*., 2011; OHZUKU *et al*., 1993; SANTOS *et al*., 2019). It means that the lamellas that form the (003) peak are composed only by cobalt ions (Figure 3). When the (003)/(104) peak intensity ratio is lower than 1.2, it is an evidence of the cationic exchange between cobalt and lithium, where cobalt, originally in a 3b site, will occupy the lithium site, 3a site, and vice versa. The calculated values for the ratio of the peak are shown in the last column for HT-LCO phase in Table 1.

Figure 3 – Crystallographic structure representation of HT-LCO phase, *R-3m* spacial group.

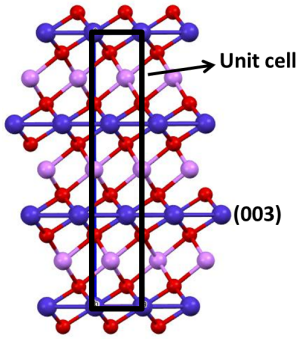

Source: The authors.

In Figure 4 the diffractograms were zoomed in the 18.00 – 20.00° 2θ region, to show in details the (003) peak, the appearance of $LiCoO_2$ phase in *Fd-3m* space group (LT-LCO), and a third phase (Li_2CO_3) from 20.00 to 35.00° (right).

Figure 4 – The graph in the left side refers to the amplification of the (003) peak for the HT phase and (111) peak for the LT phase. The contaminant Li_2CO_3 is shown on the right side of the graph.

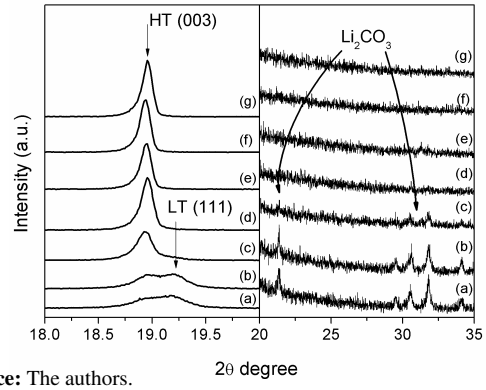

Source: The authors.

As can be seen in Figure 4 (a) and (b) the HT-LCO (003) peak is located at 18.95° while the LT-LCO (111) peak at 19.20°. In Figure 4 (c) is shown that the LT-LCO disappears but the Li_2CO_3 remains in the sample. This carbonate phase starts to disappear from 700 °C - 20 h and at 800 °C the carbonate phase disappears even in calcination time as low as 20 minutes, Figure 4 (d) to (g).

The phase weight percentage for all samples are shown in Table 1. The low-temperature LT-LCO phase seems to be in a sub-stoichiometric phase composition ($Li_{1-x}CoO_2$) since some percentage of lithium is present in the Li_2CO_3 contaminant phase. It is evident that the HT-LCO is a lithium closed phase (Li_1CoO_2) even at low treatment temperatures since the angular (003) peak position is located at 18.95° for different treatment temperatures, revealing that there were no changes in the interplanar distance. The lithium carbonate is an ionic compound and it's melting point is around 730 °C. In temperatures near to that, a reaction between Li_2CO_3 and LT-LCO occurs and the carbonate become the lithium donor to $Li_{1-x}CoO_2$ (LT phase), according to the reaction showed in equation (4) (MENG *et al*., 2019; KIM; LEE; LEE, 2008)

$$xLi_2CO_3 + 2Li_{1-x}CoO_2 \xrightarrow{\Delta} 2LiCoO_2 + CO_2 + \frac{1}{2}O_2 \quad (4)$$

Therefore it can be concluded that the carbonate phase reacts with LT-LCO phase resulting in HT-LCO phase at temperatures as higher than 700 °C.

The graph in Figure 5 shows the evolution of *FWHM* values versus the calcination temperature of each diffractogram peaks. For samples heat-treated at 600 °C the *FWHM* values are the highest and are dramatically increasing with increasing angles (2θ), which is an indication that the crystallite size is smaller and the micro-strain is higher than to the others samples. This is due to the configuration of a high disordered crystal. As the treatment temperature and time increase, the *FWHM* values decrease, as well as the curve slope. Interestingly, for temperatures of 800 °C even at the low calcination time (20 minutes), there is a tendency to the *FWHM* value saturation. In fact, samples treated at 800 °C shows *FWHM* values, in all angle range, close to the silicon standard, which allows inferring that they exhibit high crystallinity and low structural defects densities, even for the sample treated by only 20 minutes.

Table 1 – Crystallographic phase quantification, in weight percent, by Rietveld refinement, GOF is the adjust quality factor.

Sample	Crystallographic phases (wt.%)			GoF
	HT-$LiCoO_2$	**LT-$LiCoO_2$**	**Li_2CO_3**	
600 °C_1h	35.5	52.3	12.2	1.47
600 °C_20h	40.1	49.4	10.5	1.53
700 °C_1h	84.6	9.0	6.4	1.64
700 °C_20h	100.0	0	0	2.67
800 °C_20min	100.0	0	0	3.74
800 °C_1h	100.0	0	0	3.35
800 °C_20h	100.0	0	0	4.09

Source: The authors.

Figure 5 – *FWHM* values for the HT-$LiCoO_2$ phase diffraction peaks under different treatment temperatures, and for the polycrystalline silicon standard.

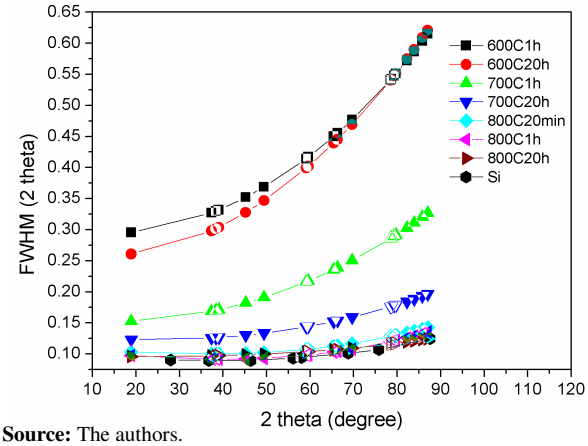

Source: The authors.

In Table 2 the lattice parameters, the c/a ratio, the peak intensity ratio ($I_{(003)}/I_{(104)}$), the crystallite size (Å) and the micro-strain (%) for all samples are presented. As reported in the literature (HU *et al.*, 2011; OHZUKU *et al.*, 1993; SANTOS *et al.*, 2019), when the c/a ratio is around 4.99 and the ($I_{(003)}/I_{(104)}$), is higher than 1.2, it indicates that the material HT-LCO may have a good electrochemical property. However, in this work all samples exhibit a value close to 4.99, thus this parameter by itself cannot be used to discriminate the samples about electrochemical performance, while the $I_{(003)}/I_{(104)}$ reveals that samples heat-treated at 700 °C and 800 °C have peak intensity ratio in the desired magnitude. As observed qualitatively in Figure 5, the values of crystallite size and micro-strain have inversely proportional behavior, while the size increase with the heat treatment, the micro-strain decrease. It is expected as the treatment temperature increase because more energy is taken to ordering the system.

As can be observed, the levels of size and strain for the samples, heat-treated at 800 °C, are enough close and may be supposed that the electrochemical performance will be high for all of them.

With the purpose to evaluate the electrochemical performance of the sample heat treated at 800 °C by 20 min, the charge/discharge cycle was performed. In Figure 6 is shown the CC-CV experiment for the 800-20min sample that shows a discharge capacity of 135 ± 10 mAh g^{-1}, with an elevated discharge potential (3.60 V vs. $Li^+|Li$). These are in good agreement with the best values for HT-LCO found in the literature, attesting that even low treatment time is enough for the sample to exhibit high electrochemical performance (DAI *et al.*, 2016; LIU *et al.*, 2017).

Figure 6 – Charge and discharge cycle of the HT-$LiCoO_2$ electrode calcined at 800 °C by 20 min.

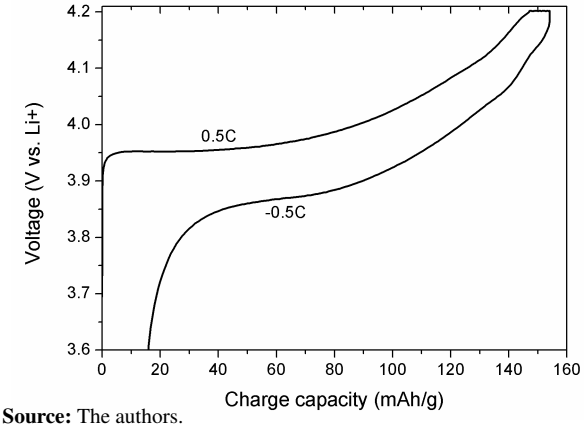

Source: The authors.

Table 2 – HT-$LiCoO_2$ data obtained from the Rietveld refinement: lattice parameters, c/a ratio, (003) and (104) peak intensity ratio, crystallite size and micro-strain.

LCO sample	**HT-$LiCoO_2$**					
	a = b [Å]	c [Å]	c/a	$I_{(003)}/I_{(104)}$	Size [Å]	Strain [%]
600 °C_1h	2.815	14.049	4.990	0.81	303.9	0.213
600 °C_20h	2.816	14.035	4.983	0.94	342.2	0.233
700 °C_1h	2.814	14.046	4.990	1.42	657.2	0.119
700 °C_20h	2.814	14.051	4.993	1.59	913.2	0.063
800 °C_20min	2.814	14.049	4.991	1.39	1225.0	0.052
800 °C_1h	2.814	14.050	4.992	1.41	1302.0	0.048
800 °C_20h	2.814	14.051	4.993	1.53	1989.0	0.025

Source: The authors.

Conclusion

In this work, the heating rate influence in the formation of high ordered $LiCoO_2$ material was evaluated. The heating rate was reduced to 5 °C min^{-1} to avoid the excessive volumetric expansion of the gel in the early stage of the synthesis, but, by doing so, the high crystallographic ordered HT-LCO was not obtained at low calcination temperature (600 °C). The HT-LCO compound requires, however, more energy than that available at 600 °C to form a pure and crystallographically well-ordered material. Nevertheless, it was demonstrated that by controlling the heating rate the HT-LCO phase is successfully synthesized at 800 °C even at a drastically reduced treatment time of only 20 min. By comparison with other works using the sol-gel synthesis reported in the literature, this scale of time is, at least, five times smaller, thus making this process time efficient and economically attractive.

References

ANTOLINI, E. $LiCoO_2$: formation, structure, lithium and oxygen nonstoichiometry, electrochemical behavior and transport properties. *Solid State Ionics*, Amsterdam, v. 170, n. 3/4, p. 159–171, 2004.

BAZITO, F. F. C.; TORRESI, R. M. Cathodes for lithium ion batteries: the benefits of using nanostructured materials. *Journal of the Brazilian Chemical Society*, São Paulo, v. 17, n. 4, p. 627–642, 2006.

BELOV, D.; YANG, M. H. Investigation of the kinetic mechanism in overcharge process for Li-ion battery. *Solid State Ionics*, Amsterdam, v. 179, n. 27/32, p. 1816–1821, 2008. Doi: <https://doi.org/10.1016/j.ssi.2008.04.031>

CHEN, H.; QIU, X.; ZHU, W.; HAGENMULLER, P. Synthesis and high rate properties of nanoparticled lithium cobalt oxides as the cathode material for lithium-ion battery. *Electrochemistry Communications*, New York, v. 4, n. 6, p. 488–491, 2002.

DAI, X. *et al*. Extending the high-voltage capacity of $LiCoO_2$ cathode by direct coating of the composite electrode with Li2CO3 via magnetron sputtering. *Journal of Physical Chemistry* C, Washington, v. 120, n. 1, p. 422–430, 2016.

DING, N.; GE, X. W.; CHEN, C. H. A new gel route to synthesize $LiCoO_2$ for lithium-ion batteries. *Materials Research Bulletin*, New York, v. 40, n. 9, p. 1451–1459, 2005.

DONG, Q.; KUMADA, N.; YONESAKI,Y.; TAKEI, T.; KINOMURA, N. Synthesis of $LiCoO_2$ via a facile hydrothermal-assisted route. *Journal of the Ceramic Society of Japan*, [Tóquio], v. 119, n. 1390, p. 538–540, 2011.

GARCIA, B; FARCY, J.; PEREIRA-RAMOS, J.P.; BAFFIER, N., Electrochemical Properties of Low Temperature Crystallized $LiCoO_2$, *Journal of The Electrochemical Society*, v. 144, issue 4, 1179-1184, 1997.

GUMMOW, R. J.; THACKERAY, M. M.; DAVID, W. I. F.; HULL, S. Structure and Electrochemistry of Lithium Cobalt Oxide. *Materials Research Bulletin*, New York, v. 27, p. 327–337, 1992.

HU, C. Y.; GUO, J.; DU, Y.; XU, H.-h.; HE, Y.-h. Effects of synthesis conditions on layered $Li[Ni_{1/3}Co_{1/3}Mn_{1/3}]O_2$ positive-electrode via hydroxide co-precipitation method for lithium-ion batteries. *Transactions of Nonferrous Metals Society of China*, [S. l.], v. 21, n. 1, p. 114–120, 2011.

JULIEN, C. 4-Volt Cathode Materials for Rechargeable Lithium Batteries Wet-Chemistry Synthesis, Structure and Electrochemistry. *Ionics*, Amsterdam, v. 6, n. 1/2, p. 30–46, 2000.

KANG, S. G.; KANG, S.Y.; RYU, K. S.; CHANG, S. H. Electrochemical and structural properties of HT-$LiCoO_2$ and LT-$LiCoO_2$ prepared by the citrate sol-gel method. *Solid State Ionics*, Amsterdam, v. 120, n. 1, p. 155–161, 1999.

KHOMANE, R. B.; AGRAWAL, A. C.; KULKARNI, B. D.; GOPUKUMAR, S.; SIVASHANMUGAM, A. Preparation and electrochemical characterization of lithium cobalt oxide nanoparticles by modified sol-gel method. *Materials Research Bulletin*, New York, v. 43, n. 8/9, p. 2497–2503, 2008. Doi: <https://doi.org/10.1016/j.materresbull.2007.08.033>

KIM, D. S.; LEE, C. K.; KIM, H. Preparation of nano-sized $LiCoO_2$ powder by the combination of sonication and modified Pechini process. *Solid State Sciences*, Paris, v. 12, n. 1, p. 45–49, 2010. Doi: <https://doi.org/10.1016/j.solidstatesciences.2009.09.022>

KIM, J.-W.; LEE, Y.-D.; LEE, H.-G. Decomposition of Li_2CO_3 by Interaction with SiO_2 in mold flux of steel continuous casting. *ISIJ International*, Tokyo, v. 44, n. 2, p. 334–341, 2008.

LI, M.; LU, J.; CHEN, Z.; AMINE, K. 30 years of lithium-ion batteries. *Advanced Materials*, Weinheim, v. 30, n. 33, p. 1–24, 2018. Doi: <https://doi.org/10.1002/adma.201800561>

LIU, A.; LIB, J.; SHUNMUGASUNDARAMA, R.; DAHNA, J. R. Synthesis of Mg and Mn doped $LiCoO_2$ and effects on high voltage cycling. *Journal of The Electrochemical Society*, Pennington, v. 164, n. 7, p. A1655–A1664, 2017.

MENG, X. *et al*. Recycling of $LiNi_{1/3}Co_{1/3}Mn_{1/3}O_2$ cathode materials from spent lithium-ion batteries using mechanochemical activation and solid-state sintering. *Waste Management*, Elmsford, v. 84, p. 54–63, 2019. Doi: <https://doi.org/10.1016/j.wasman.2018.11.034>

MIZUSHIMA, K.; JONES, P.C.; WISEMANJ, P. J.; GOODENOUGH, J. B. Li_xCoO_2 ($0 < x \leq 1$): a new cathode material for batteries of high energy density. *Solid State Ionics*, Amsterdam, v. 3/4, p. 171–174, 1981. Doi: <https://doi.org/10.1016/0025-5408(80)90012-4>

OH, I. H.; HONG, S. A.; SUN, Y. K. Low-temperature preparation of ultrafine $LiCoO_2$ powders by the sol-gel method. *Journal of Materials Science*, London, v. 32, n. 12, p. 3177–3182, 1997.

OHZUKU, T.; UEDA, A.; NAGAYAMA, M.; IWAHOSHI, Y. H. K. Comparative study of $LiCoO_2$, $LiNi_{12}Co_{12}O_2$ and $LiNiO_2$ for 4 volt secondary lithium cells. *Electrochimica Acta*, New York, v. 38, n. 9, p. 1159–1167, 1993. Doi: <https://doi.org/10.1016/0013-4686(93)80046-3>

PORTHAULT, H.; BADDOUR-HADJEAN, R.; LE CRAS, F.; BOURBON, C.; FRANGER, S. Raman study of the spinel-to-layered phase transformation in sol-gel $LiCoO_2$ cathode powders as a function of the post-annealing temperature. *Vibrational Spectroscopy*, Amsterdam, v. 62, p. 152–158, 2012. Doi: <https://doi.org/10.1016/j.vibspec.2012.05.004>

PORTHAULT, H.; LE CRAS, F.; FRANGER, S. Synthesis of $LiCoO_2$ thin films by sol/gel process. *Journal of Power Sources*, Lausanne, v. 195, n. 19, p. 6262–6267, 2010. Doi: <https://doi.org/10.1016/j.jpowsour.2010.04.058>

PREDOANĂ, L. *et al*. Electrochemical properties of the $LiCoO_2$ powder obtained by sol-gel method. *Journal of the European Ceramic Society*, Oxford, v. 27, n. 2/3, p. 1137–1142, 2007.

SANTOS, C. S. *et al*. A closed-loop process to recover Li and Co compounds and to resynthesize LiCoO2 from spent mobile phone batteries. *Journal of Hazardous Materials*, Amsterdam, v. 362, p. 458–466, 2019. Doi: <https://doi.org/10.1016/j.jhazmat.2018.09.039>

SUN, Y. K. Cycling behaviour of $LiCoO_2$ cathode materials prepared by PAA-assisted sol-gel method for rechargeable lithium batteries. Journal of Power Sources, Lausanne, v. 83, n. 1/2, p. 223–226, 1999. Doi: <https://doi.org/10.1016/S0378-7753(99)00280-3>

SUN, Y. K.; OH, I. H.; HONG, S. A. Synthesis of ultrafine $LiCoO_2$ powders by the sol-gel method. *Journal of Materials Science*, London, v. 31, n. 14, p. 3617–3621, 1996.

YOON, W. S.; LEE, K. K.; KIM, K. B. Synthesis of $LiAl_yCo_{1-y}O_2$ using acrylic acid and its electrochemical properties for Li rechargeable batteries. *Journal of Power Sources*, Lausanne, v. 97/98, p. 303–307, 2001. Doi: <https://doi.org/10.1016/S0378-7753(01)00515-8>

ZHECHEVA, E.; STOYANOVA, R; GOROVA, M.; ALCÁNTARA, R.; MORALES, J.; TIRADO, J. L. Lithium-cobalt citrate precursors in the preparation of intercalation electrode materials. *Chemistry of Materials*, Washington, v. 8, n. 7, p. 1429–1440, 1996.

ZHU, C. *et al*. High performances of ultrafine and layered $LiCoO_2$ powders for lithium batteries by a novel sol-gel process. *Journal of Alloys and Compounds*, Lausanne, v. 496, n. 1/2, p. 703–709, 2010. Doi: <https://doi.org/10.1016/j.jallcom.2010.02.178>.

Received: May 20, 2019
Accepted: Aug. 26, 2019